Environmental Science & Technology

Article

pubs.acs.org/est

Molecular Distribution and Stable Carbon Isotopic Composition of Dicarboxylic Acids, Ketocarboxylic Acids, and α-Dicarbonyls in Size-Resolved Atmospheric Particles From Xi'an City, China

Gehui Wang,*,[†,‡] Kimitaka Kawamura,[†] Chunlei Cheng,[‡] Jianjun Li,[‡] Junji Cao,[‡] Renjian Zhang,[§] Ting Zhang,[‡] Suixin Liu,[‡] and Zhuzi Zhao[‡]

[†]Institute of Low Temperature Science, Hokkaido University, Sapporo 060-0819, Japan

[‡]State Key Laboratory of Loess and Quaternary Geology, Institute of Earth Environment, Chinese Academy of Sciences, Xi'an 710079, China

[§]Institute of Atmospheric Physics, Chinese Academy of Sciences, Beijing 100029, China

Supporting Information

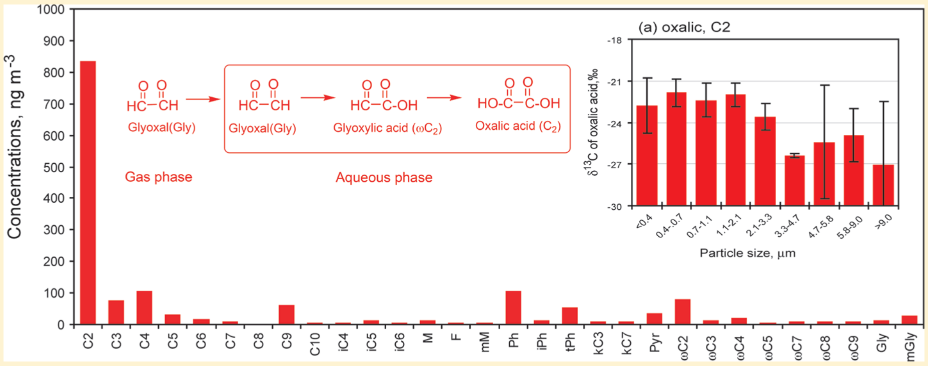

ABSTRACT: Size-resolved airborne particles (9-stages) in urban Xi'an, China, during summer and winter were measured for molecular distributions and stable carbon isotopic compositions of dicarboxylic acids, ketocarboxylic acids, and α-dicarbonyls. To our best knowledge, we report for the first time the size-resolved differences in stable carbon isotopic compositions of diacids and related compounds in continental organic aerosols. High ambient concentrations of terephthalic (tPh, 379 ± 200 ng m^{-3}) and glyoxylic acids (ωC_2, 235 ± 134 ng m^{-3}) in Xi'an aerosols during winter compared to those in other Chinese cities suggest significant emissions from plastic waste burning and coal combustions. Most of the target compounds are enriched in the fine mode (<2.1 μm) in both seasons peaking at 0.7−2.1 μm. However, summertime concentrations of malonic (C_3), succinic (C_4), azelaic (C_9), phthalic (Ph), pyruvic (Pyr), 4-oxobutanoic (ωC_4), and 9-oxononanoic (ωC_9) acids, and glyoxal (Gly) in the coarse mode (>2.1 μm) are comparable to and even higher than those in the fine mode (<2.1 μm). Stable carbon isotopic compositions of the major organics are higher in winter than in summer, except oxalic acid (C_2), ωC_4, and Ph. $\delta^{13}C$ of C_2 showed a clear difference in sizes during summer, with higher values in fine mode (ranging from −22.8‰ to −21.9‰) and lower values in coarse mode (−27.1‰ to −23.6‰). The lower $\delta^{13}C$ of C_2 in coarse particles indicate that coarse mode of the compound originates from evaporation from fine mode and subsequent condensation/adsorption onto pre-existing coarse particles. Positive linear correlations of C_2, sulfate and ωC_2 and their $\delta^{13}C$ values suggest that ωC_2 is a key intermediate, which is formed in aqueous-phase via photooxidation of precursors (e.g., Gly and Pyr), followed by a further oxidation to produce C_2.

1. INTRODUCTION

Organic aerosols account for 20−50% of airborne fine particle mass at continental midlatitudes[1,2] and as much as 90% in tropical forested regions.[3,4] Significant amounts of organic aerosols are also found in the middle troposphere.[5,6] A major fraction of organic aerosols is water-soluble, accounting for 20−60% of aerosol carbon mass in fossil fuel combustion-derived particles[7,8] and 45−75% of that in biomass burning-derived particles.[4,9] Water-soluble organic aerosols (WSOA) are hygroscopic and thus have a significant impact on climate and human health.

East Asia is a major source of anthropogenic aerosols in the world, where annual emission of anthropogenic primary organic aerosols (POA) accounts for about 10% of the total POA in the world.[10] Satellite observation showed that Guanzhong Plain in central China is one of the most heavily polluted regions in the world with an annual average $PM_{2.5}$

Received: December 6, 2011
Revised: March 30, 2012
Accepted: April 4, 2012
Published: April 4, 2012

ACS Publications © 2012 American Chemical Society

dx.doi.org/10.1021/es204322c | Environ. Sci. Technol. 2012, 46, 4783−4791

Table 1. Total Suspended Particle (TSP)-Equivalent Concentrations of Dicarboxylic Acids, Ketocarboxylic Acids, α-Dicarbonlyls, and Inorganic Ions in the Urban Air of Xi'an, Central China during Summer and Winter

	Summer (N = 3)				Winter (N = 3)			
	Min	Max	Mean	Std[a]	Min	Max	Mean	Std[a]
I. Dicarboxylic Acids, ng m^{-3}								
Oxalic, C_2	740	965	832	116	551	1529	918	532
Malonic, C_3	57	97	74	21	37	120	70	45
Succinic, C_4	99	109	104	4.8	125	307	198	96
Glutaric, C_5	26	33	30	3.5	28	75	48	24
Adipic, C_6	12	18	16	3.4	16	49	30	17
Pimelic, C_7	6.1	7.2	6.5	0.6	2.0	6.5	3.9	2.3
Suberic, C_8	0.9	1.1	1.0	0.1	0.7	2.1	1.3	0.7
Azelaic, C_9	43	72	61	15	55	142	94	44
Undecanedioic, C_{11}	2.3	5.6	4.0	1.7	2.2	9.4	5.1	3.8
Methylmalonic, iC_4	2.7	4.4	3.8	0.9	1.9	4.5	3.1	1.3
Methylsuccinic, iC_5	12	13	13	0	24	58	38	18
Methylglutaric, iC_6	4.4	5.6	5.1	0.7	5.1	12	7.7	3.5
Maleic, M	8.7	12	10	1.6	13	28	20	8
Fumaric, F	4.0	5.1	4.5	0.6	5.1	14	8.4	5.0
Methylmaleic, mM	3.0	5.1	4.0	1.1	15	32	22	9.0
Phthalic, Ph	91	121	104	15	87	246	167	79
Isophthalic, iPh	9.2	13	11	1.8	12	30	18	10
Terephthalic, tPh	50	56	52	3.7	191	590	379	200
Ketomalonic, kC_3	6.2	8.0	7.3	1.0	8.6	21	14	6.7
4-Ketopimelic, kC_7	6.3	8.2	7.0	1.0	4.1	11	7.0	3.3
Subtotal	1067	1544	1350	247	1185	3286	2053	1097
II. Ketocarboxylic Acids, ng m^{-3}								
Pyruvic, Pyr	30	42	35	6.3	32	116	66	44
Glyoxylic, ωC_2	69	83	77	7.2	128	385	235	134
3-Oxopropanoic, ωC_3	9	13	11	1.8	16	49	29	18
4-Oxobutaboic, ωC_4	17	20	18	1.9	37	91	62	27
5-Oxopentanoic, ωC_5	3.2	3.9	3.6	0.4	2.6	7.0	4.5	2.2
7-Oxoheptanoic, ωC_7	7.7	8.7	8.3	0.6	4.2	14	8.2	5.4
8−Oxooctanoic, ωC_8	5.5	8.8	7.1	1.7	4.7	15	9.2	5.4
9-Oxononanoic, ωC_9	6.1	9.0	7.4	1.5	3.1	13	7.3	5.1
Subtotal	155	184	167	15	228	690	421	240
III. α-Dicarbonyls, ng m^{-3}								
Glyoxal, Gly	12	12	12	0.2	25	76	46	27
Methylglyoxal, mGly	21	30	25	4.6	44	125	74	45
Subtotal	33	42	37	4.6	69	201	120	71
Total (all detected organics)	1260	1760	1554	259	1483	4178	2594	1409
Total/Particle mass, %	0.6	0.8	0.7	0.1	0.4	0.8	0.6	0.2
IV. Inorganic Ions, μg m^{-3}								
F^-	0.1	0.5	0.3	0.2	0.7	1.3	1.1	0.3
Cl^-	1.1	1.9	1.4	0.4	8.1	12	11	2.3
NO_3^-	14	24	18	5.1	21	44	31	12
SO_4^{2-}	37	51	42	7.7	43	80	62	19
Na^+	0.8	1.4	1.2	0.3	1.1	3.7	2.2	1.3
NH_4^+	8.8	13	11	2.1	15	27	21	6.1
K^+	0.5	1.0	0.8	0.3	1.7	3.6	2.5	0.9
Mg^{2+}	0.4	0.5	0.4	0.1	0.2	0.5	0.4	0.1
Ca^{2+}	2.1	3.5	2.6	0.8	3.8	8.4	6.4	2.4
Total	69	95	78	15	97	180	137	41
Particle mass (PM, μg m^{-3})	198	228	216	16	302	533	436	120
Total/PM, %	31	42	36	5.4	28	34	31	2.8

[a] Std: standard deviation.

of more than 80 μg m^{-3}.[11] Elemental carbon (EC) and organic carbon (OC) in Guanzhong Plain were reported as high as 29 ± 8.9 and 125 ± 55 μg m^{-3} respectively in winter due to fossil fuel and biofuel combustion for house heating.[12,13] Guanzhong Plain is located in a semiarid region where precipitation is inactive and wind speed is low due to its basinlike topography. It was reported that high level of $PM_{2.5}$ in this region resulted in significant impairment on visibility and human health,[14] in which WSOA may take an important role since they not only scatter/absorb visible

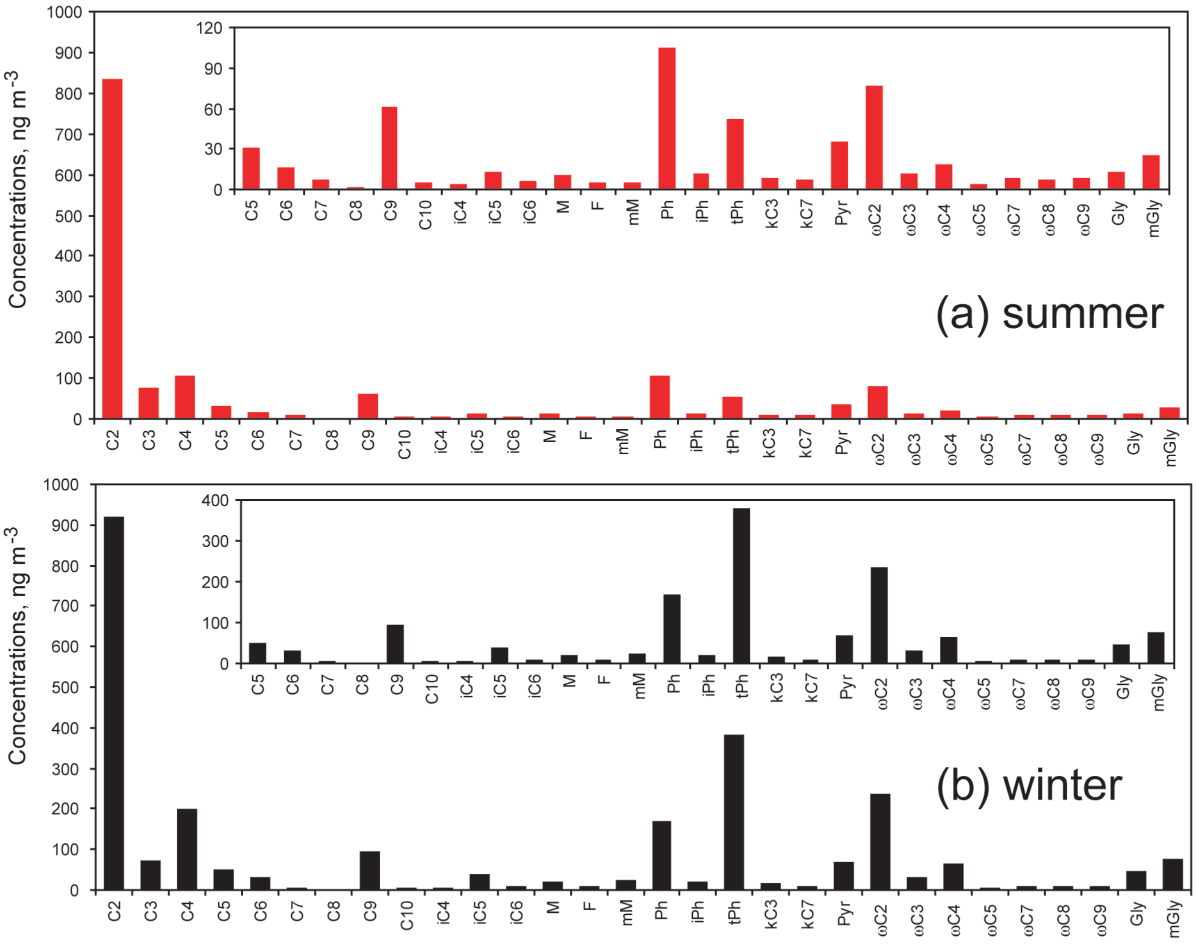

Figure 1. Seasonal variations of molecular distributions of dicarboxylic acids and related compounds in total suspended particles of Xi'an, central China during (a) summer and (b) winter.

light but also increase the solubility of pollutants in the human respiratory tract.[15,16]

Dicarboxylic acids are important components of WSOA, which have been found ubiquitously in the atmosphere. In this study, we first measure dicarboxylic acids (C_2−C_9), ketocarboxylic acids and α-dicarbonyls on a molecular level in size-resolved particles collected in Xi'an, a mega-city in Guanzhong Plain, and then determine stable carbon isotopic composition of the above individual organic compounds in the size-segregated aerosols to investigate their sources and formation mechanisms.

2. EXPERIMENTAL SECTION

2.1. Sample Collection. Size-segregated aerosols were collected in the urban area of Xi'an using a 9-stage impactor equipped with precombusted quartz fiber filter (Whatman 41, ϕ 90 mm, 450 °C for 8 h) at an airflow rate of 28 L/min. The sampler was set on the rooftop of a two-story building. The 50% cutoff sizes are <0.4, 0.4−0.7, 0.7−1.1, 1.1−2.1, 2.1−3.3, 3.3−4.7, 4.7−5.8, 5.8−9.0, and ≥9.0 μm. The airflow was calibrated before and after sampling using an airflow meter supplied by the sampler manufacturer to keep the sampler working at the specified flow rate. Three sets of samples were collected in the summer and winter of 2009, respectively. Each set of samples was continuously collected for 5 days. After a 48 h equilibration in a glass chamber (25 ± 0.5 °C, RH 40 ± 2%), each samples was measured three times for particle mass (PM) with the difference less than 3%. The summer sampling was performed on July 15th−August second and the winter sampling was performed on November 14th−30th. One set of field blanks was also collected in each season after the sampling. The summer sampling was stopped for a few days due to raining. Meteorological conditions during the sampling time were summarized in Table S1 of the Supporting Information. Wintertime house heating in Guanzhong Plain lasts each year from November 15th to March 15th resulting in a severe haze period during the sampling campaign with visibility down to less than 1 km (Table S1 of the Supporting Information).

2.2. Sample Analysis. *a). Inorganic Ions.* One-fourth of the filter was cut into pieces, extracted 3 times each with 5 mL Milli-Q water under sonication and filtered using a PTFE filter to remove any particles and filter debris. The combined extraction was determined by Dionex 600 ion chromatography.[5]

b). Dicarboxylic Acids, Ketocarboxylic Acids, and α-Dicarbonyls. Another one-fourth filter was also extracted with Milli-Q water. After extraction, pH of the extracts was adjusted into 8.5−9.0 using a 0.1 M KOH solution to convert carboxylic acids into corresponding salts for improving the recoveries of smaller diacids (e.g., oxalic acid). Then the sample was concentrated into dryness using a rotary evaporator under vacuum, and reacted with 14% BF_3/butanol (300 μL) at 100 °C for 1 h. After the reaction, acetonitrile (300 μL) and *n*-hexane

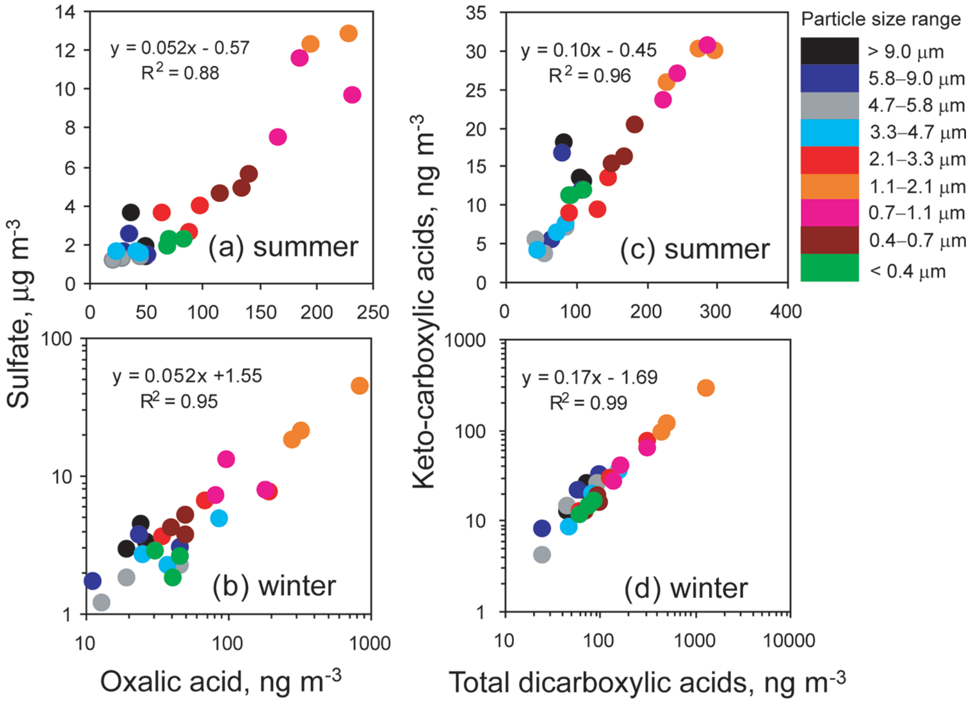

Figure 2. Linear fit regression for oxalic acid with sulfate (a and b) and dicarboxylic acids with ketocarboxylic acids (c and d) on each stage.

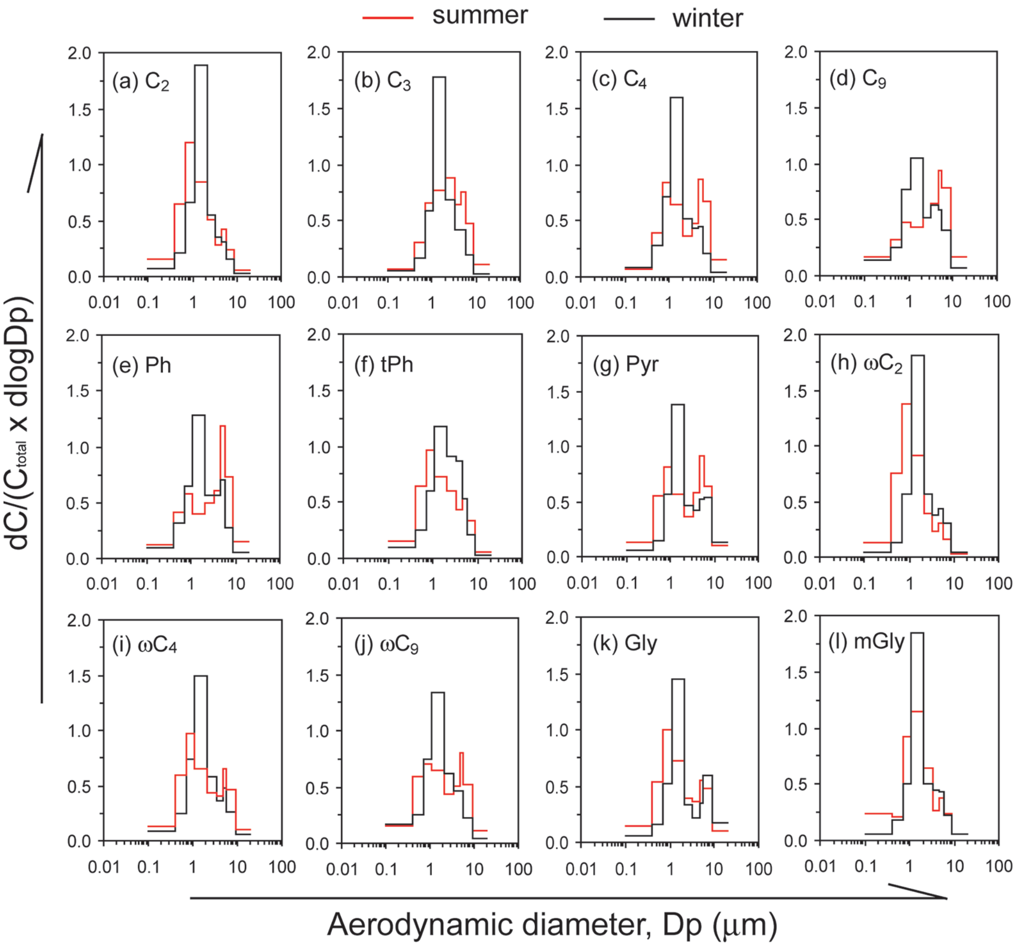

Figure 3. Size distributions of dicarboxylic acids and related compounds in Xi'an during summer and winter.

(5 mL) were added into the derivatized sample, and extracted with Milli-Q water (5 mL) 3 times. The hexane layer was further concentrated into 100 μL prior to GC and GC/MS analysis.[17] Diacids and related compounds were quantified by a

gas chromatography equipped with a FID detector. GC oven temperature was increased from 50 °C (2 min) to 120 °C at a rate of 15 °C min^{-1}, and then to 310 °C at a rate of 5 °C min^{-1} and held for 15 min. The target compounds were also confirmed using a GC/MS technique. Compared to previous studies,[17,18] recoveries of diacids and related compounds are improved; 90–93% for oxalic acid and 96–110% for others.

c). Stable Carbon Isotopic Composition of Diacids and Related Compounds. Stable carbon isotopic compositions ($\delta^{13}C$) of the water-soluble compounds relative to Pee Dee Belemnite (PDB) were measured using the method developed by Kawamura and Watanabe.[19] Briefly, $\delta^{13}C$ values of the derivatives were determined using GC (HP6890)/isotope ratio mass spectrometry (irMS) (Finnigan-MAT Delta plus). The $\delta^{13}C$-values were then calculated for free organic acids using an isotopic mass balance equation based on the measured $\delta^{13}C$ of the derivatives and derivatizing agent (1-butanol).[19] Each sample was analyzed for 2–3 times to ensure the difference in $\delta^{13}C$ values less than 1‰. $\delta^{13}C$ of the quantified compound in the three set samples in each season are averaged and reported here.

Table 2. Relative Abundances of Major Organic Compounds in Fine (<2.1μm) and Coarse (>2.1μm) modes[a], %

	Summer		Winter	
	Fine	Coarse	Fine	Coarse
I. Dicarboxylic Acids				
C_2	72 ± 3.3	28 ± 3.3	76 ± 4.2	24 ± 4.2
C_3	46 ± 4.1	54 ± 4.1	70 ± 4.5	30 ± 4.5
C_4	49 ± 7.3	51 ± 7.3	71 ± 4.0	29 ± 4.0
C_9	39 ± 1.7	61 ± 1.7	61 ± 10	39 ± 10
Ph	40 ± 2.8	60 ± 2.8	63 ± 4.5	37 ± 4.5
tPh	64 ± 0.5	36 ± 0.5	57 ± 1.0	43 ± 1.0
II. Ketocarboxylic Acids				
Pyr	54 ± 11	46 ± 11	57 ± 10	43 ± 10
ωC_2	61 ± 5.7	39 ± 5.7	70 ± 7.5	30 ± 7.5
ωC_4	59 ± 1.9	41 ± 1.9	63 ± 4.2	37 ± 4.2
ωC_9	71 ± 6.5	29 ± 6.5	69 ± 7.3	31 ± 7.3
III. α-Dicarbonyls				
Gly	56 ± 5.8	44 ± 5.8	57 ± 8.1	43 ± 8.1
mGly	70 ± 8.6	30 ± 8.6	67 ± 5.8	33 ± 5.8

[a] For compound abbreviation, see Table 1.

3. RESULTS AND DISCUSSION

3.1. Seasonal Differences in Molecular Compositions and Concentrations.

a). Dicarboxylic Acids. Concentrations

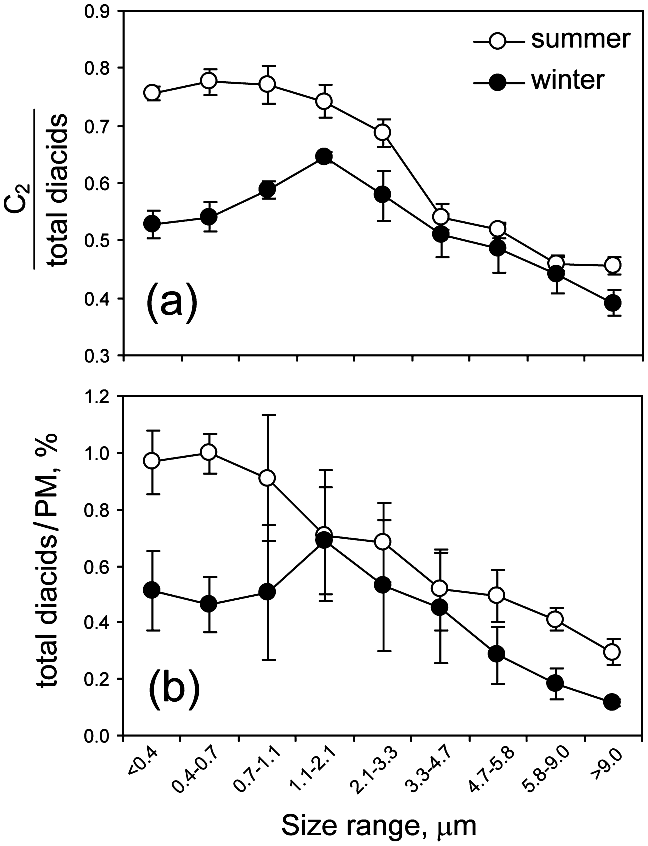

Figure 4. Relative abundance of diacids on each stage (a) oxalic acid (C_2) to total diacids, (b) total diacids to particle mass (PM).

Table 3. Geometric Mean Diameters (GMD, μm) of Major Organic Compounds in Fine (<2.1 μm) and Coarse (>2.1 μm) Modes during Summer and Winter[a]

	Summer		Winter		Winter/Summer[b]	
	Fine	Coarse	Fine	Coarse	Fine	Coarse
I. Dicarboxylic Acids						
C_2	0.82 ± 0.02	5.46 ± 0.17	1.17 ± 0.10	4.71 ± 0.59	1.43	0.86
C_3	0.96 ± 0.06	5.72 ± 0.33	1.19 ± 0.10	4.78 ± 0.58	1.25	0.84
C_4	0.88 ± 0.06	7.66 ± 0.33	1.09 ± 0.09	5.25 ± 0.58	1.24	0.69
C_9	0.67 ± 0.04	7.28 ± 0.46	0.91 ± 0.09	6.04 ± 0.64	1.35	0.83
Ph	0.71 ± 0.03	6.98 ± 0.78	1.01 ± 0.07	5.36 ± 0.48	1.43	0.77
tPh	0.78 ± 0.06	5.33 ± 0.29	1.01 ± 0.08	4.15 ± 0.15	1.30	0.78
II. Ketocarboxylic Acids						
Pyr	0.77 ± 0.05	7.69 ± 1.54	1.15 ± 0.10	6.55 ± 1.22	1.51	0.85
ωC_2	0.86 ± 0.02	7.68 ± 0.84	1.24 ± 0.10	5.64 ± 0.82	1.44	0.73
ωC_4	0.79 ± 0.03	6.85 ± 0.79	0.97 ± 0.08	6.18 ± 0.46	1.22	0.90
ωC_9	0.85 ± 0.09	5.22 ± 1.30	0.89 ± 0.22	5.09 ± 0.76	1.05	0.98
III. α-Dicarbonyls						
Gly	0.86 ± 0.07	9.30 ± 0.34	1.17 ± 0.10	6.74 ± 1.12	1.35	0.72
mGly	0.96 ± 0.07	5.65 ± 1.55	1.20 ± 0.14	5.65 ± 1.03	1.25	1.00

[a] For compound abbreviation, see Table 1. [b] Ratio of GMD in winter to that in summer.

Table 4. Stable Carbon Isotopic Composition ($\delta^{13}C$, ‰)[a] of Major Compounds in Different Size Ranges

Size range, μm	<0.4	0.4–0.7	0.7–1.1	1.1–2.1	2.1–3.3	3.3–4.7	4.7–5.8	5.8–9.0	>9.0
I. Summer ($N = 3$)									
Oxalic acid, C_2	−22.8 ± 2.0	−21.9 ± 1.0	−22.4 ± 1.2	−22.0 ± 0.8	−23.6 ± 1.0	−26.4 ± 0.2	−25.4 ± 4.1	−24.9 ± 1.9	−27.1 ± 4.5
Succinic acid, C_4	na[b]	−23.0 ± 1.4	−25.6 ± 2.2	−23.5 ± 2.7	na	−21.0	−16.7	−22.6 ± 0.1	−23.3 ± 0.2
Glyoxylic acid, ωC_2	−46.7 ± 12.2	−34.3 ± 1.5	−43.4 ± 7.6	−44.0 ± 1.1	−49.2 ± 14.0	−57.9	−62.9 ± 5.7	−46.6 ± 6.1	−42.4 ± 8.1
4-Oxobutanoic acid, ωC_4	na	−28.9 ± 4.1	−34.4 ± 2.6	−25.3 ± 6.1	−29.3	na	na	−26.3	−25.9 ± 1.8
Pyruvic acid, Pyr	−24.0	−26.7 ± 1.5	−30.1 ± 3.8	−27.9 ± 7.1	−32.7	−44.6	na	−29.0	−25.8 ± 4.1
Glyoxal, Gly	na	−36.8	−26.8 ± 2.3	−21.5 ± 0.0	−29.0	na	na	na	−30.3
Phthalic acid, Ph	−31.4 ± 0.2	−28.8 ± 0.7	−31.7 ± 2.1	−30.7 ± 3.6	−32.2 ± 5.4	−34.7 ± 3.5	−31.4 ± 3.7	−29.0 ± 1.3	−31.2 ± 5.1
II. Winter ($N = 3$)									
Oxalic acid, C_2	−23.5 ± 2.4	−21.1 ± 1.1	−22.3 ± 0.9	−21.8 ± 0.8	−24.2 ± 1.4	−22.9 ± 0.8	−22.4 ± 1.6	−24.1 ± 1.5	−25.2 ± 2.8
Succinic acid, C_4	−16.4	−15.0 ± 0.2	−16.7 ± 2.7	−17.7 ± 1.6	−16.9	−18.0	−15.4	−16.3	−14.9
Glyoxylic acid, ωC_2	−46.3 ± 14.7	−38.2 ± 18.1	−25.3 ± 9.7	−24.7 ± 3.4	−25.1 ± 1.7	−25.9 ± 12.2	−28.4 ± 3.6	−35.4 ± 9.7	−32.4 ± 6.0
4-Oxobutanoic acid, ωC_4	−22.8 ± 3.6	−30.5 ± 3.8	−25.2 ± 0.6	−26.4 ± 4.9	−24.1 ± 1.8	−31.8 ± 3.9	−26.6	−27.9 ± 0.2	−25.6 ± 3.5
Pyruvic acid, Pyr	−21.4	−28.1	na	−21.5 ± 0.6	−21.6	−21.9 ± 7.4	−20.7	−24.6 ± 5.7	−22.7 ± 1.6
Glyoxal, Gly	−18.2	−24.0 ± 7.5	−14.8 ± 4.0	−15.4 ± 2.5	−14.9	na	−22.4	−25.6 ± 5.4	−28.0 ± 3.1
Phthalic acid, Ph	−33.1 ± 1.0	−29.7 ± 1.2	−29.1 ± 1.4	−30.8 ± 4.0	−32.5 ± 2.3	−32.0 ± 5.3	−34.1 ± 1.5	−42.4 ± 3.0	−31.7 ± 2.0

[a] Numbers with a standard deviation mean that the compound isotopic composition was measured twice or three times, whereas the numbers without a standard deviation means the compound isotopic composition was measured only once due to lower amounts. [b] Not available due to low concentrations.

of dicarboxylic acids, ketocarboxylic acids, α-dicarbonyls, and inorganic ions in each size-range are summarized as total suspended particle (TSP)-equivalent concentrations and shown in Table 1. Seasonal difference in molecular compositions of diacids and related compounds is illustrated in Figure 1. As shown in part a of Figure 1, concentration order of major identified organic compounds in summer is $C_2 > C_4 \approx Ph > \omega C_2 \approx C_3 > C_9 > tPh > Pyr$ (compound abbreviation in Table 1, thereafter). In contrast, the order in winter is $C_2 > tPh > \omega C_2 > C_4 > Ph > C_3 > Pyr$ (part b of Figure 1). Such a difference in molecular composition is mostly caused by an enhanced emission from burning coal, biofuel, and plastic wastes for house heating.[12,13] Oxalic acid, the smallest dicarboxylic acid in aerosol phase, ranged from 551−1529 ng m^{-3} with an average of 918 ± 532 ng m^{-3} in winter, being similar to that in summer (Table 1).

Sulfate and oxalic acid in each size range showed a strong linear correlation in summer ($r^2 = 0.88$, part a of Figure 2) and winter ($r^2 = 0.95$, part b of Figure 2). Such a size-independent correlation indicates that both species are largely formed via a similar formation pathway, for example, an aqueous-phase oxidation.[20] C_2 in aerosols is an end product of many precursors including low molecular weight diacids, thus relative abundance of C_2/total diacids is indicative of aerosol aging. C_2/total diacids is 0.62 ± 0.01 in summer and 0.43 ± 0.04 in winter suggesting that summer aerosols are more oxidized due to more efficient photooxidation. Concentration ratio of C_6/C_9 is 0.26 ± 0.02 in summer and 0.32 ± 0.03 in winter implying an increased emission from coal burning and/or a decreased emission from plants during winter since C_6 is produced via photodegradation of anthropogenic cyclohexane[21,22] and C_9 is an photooxidation product of unsaturated fatty acids from plant emissions.[23] Naphthalene is a major precursor of phthalic acid in urban area,[24] which is photochemically oxidized to phthalic acid in gas phase and subsequently condensed/adsorbed onto preexisting aerosols. Terephthalic acid (tPh) is an important industrial material used for plastic production such as polyester fiber and PET (polyethyleneterephthalate) thermoplastics, which can be directly produced when burning plastic wastes.[25] Concentration (52 ± 3.7 ng m^{-3}, Table 1) of tPh in summer is only a half of Ph, but twice higher than Ph in winter. The wintertime concentration (379 ± 200 ng m^{-3}, Table 1) of tPh is about 7 times higher than that in summer. Such a seasonal variation indicates an importance of open and domestic burning of plastic materials in the city and the surroundings especially in cold season.

b). Ketocarboxylic Acids. Ketocarboxylic acids showed a predominance of glyoxylic acid (ωC_2) in both summer and winter samples, followed by Pyr, ωC_4 and ωC_3 (Figure 1). Concentrations of ketoacids in summer were twice lower than those in winter (Table 1). A strong linear correlation was also found between ketocarboxylic acids and total dicarboxylic acids in each stage for both seasons (parts c and d of Figure 2). Such a size-independent correlation may suggest that ketocarboxylic acids are intermediates of dicarboxylic acids. Because ωC_2 and oxalic acid (C_2) during the two seasons showed a robust linear correlation with $r > 0.92$ and both well correlated with sulfate, it is very likely that C_2 in Xi'an is largely produced by aqueous-phase oxidation of ωC_2 in aerosols. Such a C_2 production is more efficient in summer due to higher temperature (Table S1 of the Supporting Information)[26] resulting in $C_2/\omega C_2$ ratio higher in summer (11 ± 1.8, calculated from Table 1) than in winter (3.9 ± 0.4).

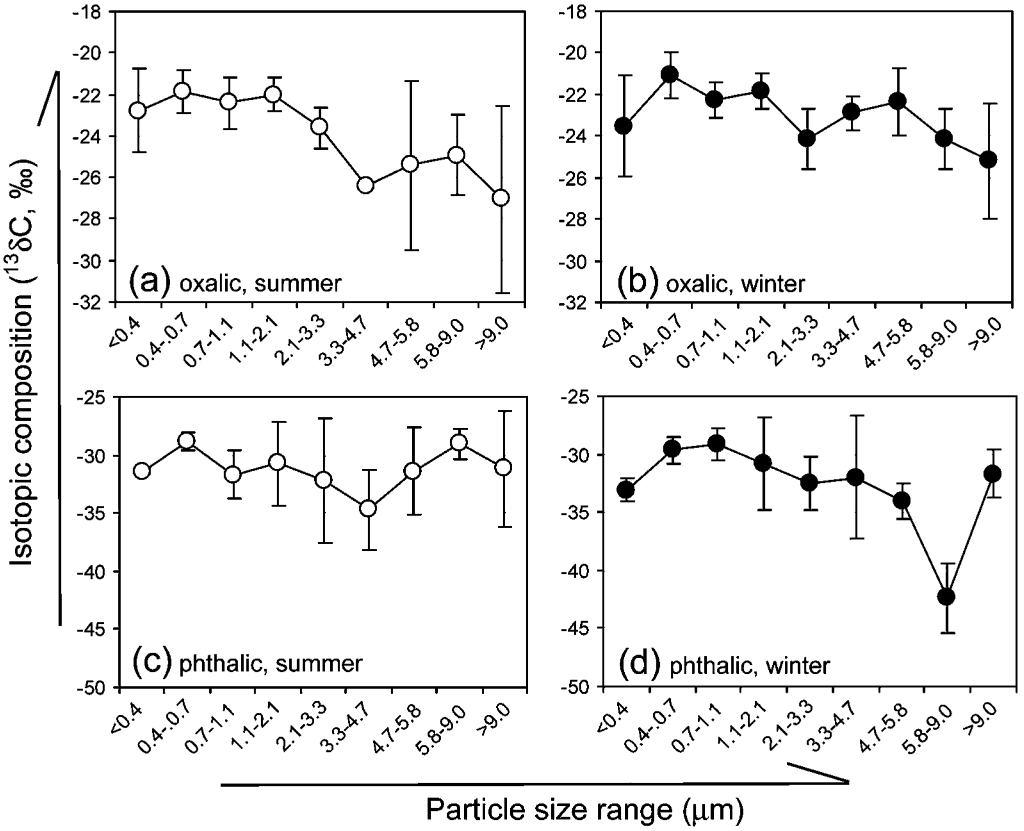

Figure 5. $\delta^{13}C$ of oxalic and phthalic acids as a function of particle sizes in Xi'an, China, during summer and winter.

c). α-Dicarbonyls. Glyoxal (Gly) and methylglyoxal (mGly) are the two smallest dicarbonyls in the atmosphere, and are formed via photochemical oxidation of biogenic (e.g., isoprene, monoterpenes) and anthropogenic volatile organic compounds (VOCs) (e.g., aromatics, acetone, and acetylene).[27,28] Both carbonyls can partition into aerosol phase and further be oxidized to form less-volatile organic acids such as pyruvic acid, ωC_2, and C_2.[29] Concentrations of Gly and mGly were 12 ± 0.2 and 25 ± 4.6 ng m^{-3} in summer and increased to 46 ± 27 and 74 ± 45 ng m^{-3} in winter, respectively (Table 1). The enhanced concentration in winter is most likely due to the high emission of their precursors (e.g., aromatics) from coal burning for house heating, because both compounds also well correlate with sulfate and Ph ($r = 0.77-0.96$, Table S2 of the Supporting Information) and O_3 level in this region is much lower in winter than in summer.[30] All of the detected organics together with inorganic ions accounted for 37 ± 5.8% and 32 ± 3.1% of particle mass in summer and winter respectively with the remaining largely being EC, mineral dust, and other unidentified organics (Table 1).

3.2. Size Distribution. Seasonal differences in the size distribution of all the target organic and inorganic compounds were investigated. Here, we will focus on selected major species. As shown in Table S2 of the Supporting Information, all of the species in each size range well correlate with one another in winter with a correlation coefficient (r) > 0.77. Atmospheric SO_4^{2-} and F^- in China are mostly derived from coal burning emissions.[5] Therefore, such strong correlations in all stages, together with the wintertime increases in the concentrations of $SO_4^{2-}$and F^-, further indicate that emissions of coal burning for house heating dominate the precursors of these organics in Xi'an. Figure 3 shows the detailed size distribution of major species. During winter C_2, C_3, C_4, tPh, ωC_2, ωC_9, and mGly showed a unimodal pattern peaking at the size range of 1.1–2.1 μm (parts a, b, c, f, h, j, and l of Figure 3). In contrast, other species such as C_9, Ph, Pyr, ωC_4, and Gly in winter showed a bimodal pattern with a large peak in the size range of 1.1–2.1 μm and a small/minor peak in the size larger than 3.3 μm (parts d,e, g, i, and k of Figure 3). However, in summer a bimodal pattern was found for most of these species, except for C_2, C_3, tPh, and ωC_2, with two peaks at the sizes of 0.7–1.1 μm and >3.3 μm (parts a–l of Figure 3).

Size distribution patterns of C_2 in the two seasons are same as those of ωC_2, along with a similar pattern found for C_4 and ωC_4 in both seasons, further suggesting that oxalic (C_2) and succinic (C_4) acids are produced via aerosol phase oxidation of ωC_2 and ωC_4. C_9 is a photooxidation product of unsaturated fatty acids (e.g., $C_{18:1}$).[23] Unsaturated fatty acids are emitted directly as fine particles from cooking activity and coarse particles from plant surfaces via wind abrasion. Thus, a bimodal pattern of C_9 was observed in both seasons (part d of Figure 3). Compared to that in winter, an enhanced concentration of C_9 in the coarse mode (>3.3 μm) in summer indicates more significant plant emissions.[31,32] Unlike in winter, Ph is enriched in coarse mode in summer (part e of Figure 3), which can be explained by an enhanced adsorption of gaseous phthalic acid produced by a gas-phase photo-oxidation of naphthalene.[31,33] tPh mostly originates from burning plastic wastes, thus showed a similar pattern in both seasons (part f of Figure 3).

Relative abundances of all the organic compounds in fine mode (<2.1 μm) except tPh, ωC_9, and mGly are lower in summer than in winter (Table 2). This can be explained in part by an increased evaporation into the air from fine particles and subsequent adsorption onto coarse particles during summer, resulting in geometric mean diameters (GMDs) of the compounds smaller in fine mode and larger in coarse mode in the hot season (Table 3).[5,34−36] Moreover, the larger fine mode of GMD in winter is also in part attributed to an enhanced hygroscopic growth since relative humidity is high and sulfate in fine mode is much more abundant compared to those in summer (Table S1 of the Supporting Information and parts a and b of Figure 2). As seen in Figure 4, concentration ratios of C_2/total diacids and diacids/PM (particle mass) in each size range are larger in summer than that in winter, again demonstrating that aerosols are more oxidized in summer.

3.3. Stable Carbon Isotopic Composition. Table 4 shows $\delta^{13}C$ values of major dicarboxylic acids and related compounds on each stage. $\delta^{13}C$ values of C_2, ωC_4 and Ph in each size range are similar in both seasons, but those of C_4, ωC_2, Pyr, and Gly are generally lower in summer than in winter. Because the $\delta^{13}C$ value of coal is larger than that of petroleum fuel,[37,38] the ^{13}C enrichments of these aerosols in winter can be ascribed to an increased emission of coal burning. Figure 5 plots the $\delta^{13}C$ values of C_2 and Ph as a function of particle size. A clear difference in $\delta^{13}C$ between the fine and coarse modes was found for C_2 in summer (part a of Figure 5). As mentioned above, C_2 is formed in aqueous phase by a photo-oxidation of ωC_2 and enriched in fine particles. The fine mode C_2 may evaporate into the air and subsequently condense/adsorb onto coarse particles resulting in the C_2 retained in fine particles more enriched with ^{13}C due to kinetic isotope effects (KIEs).[17,39,40] Compared to that in winter, such a shift from fine particles to coarse particles is more efficient in summer due to higher temperature (22−37 °C in summer versus −4−10 °C in winter, Table S1 of the Supporting Information), therefore, the higher concentration of C_2 in coarse mode (part a of Figure 3) and the more significant difference in $\delta^{13}C$ were found in summer.

ωC_2 is a product of aqueous phase photo-oxidation of precursors including Gly, mGly, Pyr, glycolic acid, and acetic acid.[26] During irreversible chemical reactions, lighter isotope (^{12}C) is preferentially enriched in the reaction products due to KIEs,[39] thus ωC_2 on each stage in both seasons showed more negative $\delta^{13}C$ values compared to those of Gly and Pyr (Table 4). As mentioned above, C_4 is most likely formed via an aqueous-phase oxidation of ωC_4 and other larger compounds. During the degradation process, these precursors can be oxidized into C_4 and release of CO_2/CO[17] resulting in the remaining substrate (e.g., C_3 and C_4) more enriched in ^{13}C (Table 4). C_3 and C_4 can further be oxidized into C_2,[18] therefore, $\delta^{13}C$ value of the total C_2 is dependent on the relative contributions from ωC_2, C_3 and C_4.

■ ASSOCIATED CONTENT

Ⓢ Supporting Information

Meteorological conditions during the sampling periods, and correlation coefficients of major identified species. This material is available free of charge via the Internet at http://pubs.acs.org.

■ AUTHOR INFORMATION

Corresponding Author

*Tel: 86-29-8832-9320, fax: 86-29-8832-0456, e-mail: wanggh@ieecas.cn, or gehuiwang@yaoo.com.cn.

Notes

The authors declare no competing financial interest.

■ ACKNOWLEDGMENTS

This work was supported by China Natural Science Foundation (No. 40873083), the Knowledge Innovation Program of Chinese Academy of Sciences (No. KZCX2-YW-148), and Environment Research and Technology Development Fund (B-0903) from the Ministry of Environment, Japan. We are also grateful to Institute of Low Temperature Science of Hokkaido University, Japan, for a financial support to G. Wang. We thank E. Tachibana for her technical assistance of GC/irMS analyses.

■ REFERENCES

(1) Zhang, Q.; Jimenez, J. L.; Canagaratna, M. R.; Allan, J. D.; Coe, H.; Ulbrich, I.; Alfarra, M. R.; Takami, A.; Middlebrook, A. M.; Sun, Y. L.; Dzepina, K.; Dunlea, E.; Docherty, K.; DeCarlo, P. F.; Salcedo, D.; Onasch, T.; Jayne, J. T.; Miyoshi, T.; Shimono, A.; Hatakeyama, S.; Takegawa, N.; Kondo, Y.; Schneider, J.; Drewnick, F.; Borrmann, S.; Weimer, S.; Demerjian, K.; Williams, P.; Bower, K. N.; Bahreini, R.; Cottrell, L.; Griffin, R. J.; Rautiainen, J.; Sun, J. Y.; Zhang, Y. M.; Worsnop, D. R. Ubiquity and dominance of oxygenated species in organic aerosols in anthropogenically-influenced Northern Hemisphere midlatitudes. *Geophys. Res. Lett.* **2007**, *34*, L13801 DOI: 10.1029/2007GL029979.

(2) Kanakidou, M.; Seinfeld, J. H.; Pandis, S. N.; Barnes, I.; Dentener, F. J.; Facchini, M. C.; Van Dingenen, R.; Ervens, B.; Nenes, A.; Nielsen, C. J.; Swietlicki, E.; Putaud, J. P.; Balkanski, Y.; Fuzzi, S.; Horth, J.; Moortgat, G. K.; Winterhalter, R.; Myhre, C. E. L.; Tsigaridis, K.; Vignati, E.; Stephanou, E. G.; Wilson, J. Organic aerosol and global climate modelling: A review. *Atmos. Chem. Phys.* **2005**, *5*, 1053−1123.

(3) Andreae, M. O.; Andreae, T. W.; Annegarn, H.; Beer, J.; Cachier, H.; leCanut, P.; Elbert, W.; Maenhaut, W.; Salma, I.; Wienhold, F. G.; Zenker, T. Airborne studies of aerosol emissions from savanna fires in southern Africa: 2. Aerosol chemical composition. *J. Geophys. Res.* **1998**, *103* (D24), 32119−32128.

(4) Falkovich, A. H.; Graber, E. R.; Schkolnik, G.; Rudich, Y.; Maenhaut, W.; Artaxo, P. Low molecular weight organic acids in aerosol particles from Rondonia, Brazil, during the biomass-burning, transition and wet periods. *Atmos. Chem. Phys.* **2005**, *5*, 781−797.

(5) Wang, G.; Li, J.; Chen, C.; Hu, S.; Xie, M.; Gao, S.; Zhou, B.; Dai, W.; Cao, J.; An, Z. Observation of atmospheric aerosols at Mt. Hua and Mt. Tai in central and east China during spring 2009-Part 1. EC, OC and inorganic ions. *Atmos. Chem. Phys.* **2011**, *11*, 4221−4235.

(6) Wang, G. H.; Kawamura, K.; Hatakeyama, S.; Takami, A.; Li, H.; Wang, W. Aircraft measurement of organic aerosols over China. *Environ. Sci. Technol.* **2007**, *41*, 3115−3120.

(7) Pathak, R. K.; Wang, T.; Ho, K. F.; Lee, S. C. Characteristics of summertime PM2.5 organic and elemental carbon in four major Chinese cities: Implications of high acidity for water-soluble organic carbon (WSOC). *Atmos. Environ.* **2011**, *45* (2), 318−325.

(8) Miyazaki, Y.; Kondo, Y.; Takegawa, N.; Komazaki, Y.; Kawamura, K.; Mochida, M.; Okuzawa, K.; Weber, R. J. Time-resolved measurements of water-soluble organic carbon in Tokyo. *J. Geophys. Res.* **2006**, *111*, D23206 DOI: 10.1029/2006JD007125.

(9) Graham, B.; Mayol-Bracero, O. L.; Guyon, P.; Roberts, G. C.; Decesari, S.; Facchini, M. C.; Artaxo, P.; Maenhaut, W.; Koll, P.; Andreae, M. O. Water-soluble organic compounds in biomass burning aerosols over Amazonia - 1. Characterization by NMR and GC-MS. *J. Geophys. Res. Atmos.* **2002**, *107*, D20 DOI: 10.1029/2001JD000336.

(10) Bond, T. C.; Streets, D. G.; Yarber, K. F.; Nelson, S. M.; Woo, J. H.; Klimont, Z. A technology-based global inventory of black and organic carbon emissions from combustion. *J. Geophys. Res. Atmos.* **2004**, *109*, D14203 DOI: 10.1029/2003JD003697.

(11) van Donkelaar, A.; Martin, R. V.; Brauer, M.; Kahn, R.; Levy, R.; Verduzco, C.; Villeneuve, P. J. Global estimates of ambient fine particulate matter concentrations from satellite-based aerosol optical depth: development and application. *Environ. Health Perspect.* **2010**, *118*, 8347−8355.

(12) Wang, G. H.; Kawamura, K.; Lee, S. C.; Ho, K. F.; Cao, J. J. Molecular, seasonal and spatial distributions of organic aerosols from fourteen Chinese cities. *Environ. Sci. Technol.* **2006**, *40*, 4619−4625.

(13) Cao, J. J.; Chow, J. C.; Lee, S. C.; Li, Y.; Chen, S. W.; An, Z. S.; Fung, K.; Watson, J. G.; C.S, Z.; Liu, S. X. Characterization and source apportionment of atmospheric organic and elemental carbon during fall and winter of 2003 in Xi'an, China. *Atmos. Chem. Phys.* **2005**, *5*, 3127−3137.

(14) Cao, J.; Xu, H.; Xu, Q.; Chen, B.; Kan, H. Fine particulate matter constituents and cardiopulmonary mortality in a heavily polluted Chinese city. *Environ. Health Perspect.* **2012**, *120*, 373−378.

(15) Glotfelty, D. E.; Seiber, J. N.; Liljedahl, L. A. Pesticides in fog. *Nature* **1987**, *325*, 602−605.

(16) Kroll, J. H.; Seinfeld, J. H. Chemistry of secondary organic aerosol: Formation and evolution of low-volatility organics in the atmosphere. *Atmos. Environ.* **2008**, *41*, 3593−3624.

(17) Aggarwal, S. G.; Kawamura, K. Molecular distributions and stable carbon isotopic compositions of dicarboxylic acids and related compounds in aerosols from Sapporo, Japan: Implications for photochemical aging during long-range atmospheric transport. *J. Geophys. Res. Atmos.* **2008**, *113*, D14301 DOI: 10.1029/2007JD009365.

(18) Kawamura, K.; Umemoto, N.; Mochida, M.; Bertram, T.; Howell, S.; Huebert, B. J., Water-soluble dicarboxylic acids in the tropospheric aerosols collected over east Asia and western North Pacific by ACE-Asia C-130 aircraft. *J. Geophys. Res. Atmos.* **2003**, *108* (D23), doi:10.1029/2002JD003256.

(19) Kawamura, K.; Watanabe, T. Determination of stable carbon isotopic compositions of low molecular weight dicarboxylic acids and ketocarboxylic acids in atmospheric aerosol and snow samples. *Anal. Chem.* **2004**, *76* (19), 5762−5768.

(20) Yu, J. Z.; Huang, X. F.; Xu, J. H.; Hu, M. When aerosol sulfate goes up, so does oxalate: Implication for the formation mechanisms of oxalate. *Environ. Sci. Technol.* **2005**, *39* (1), 128−133.

(21) Grosjean, D.; Cauwenberghe, K. V.; Schmid, J. P.; Kelly, P. E.; Pitts, J. N., Jr Identification of C3-C10 aliphatic dicarboxylic acids in airborne particulate matter. *Environ. Sci. Technol.* **1978**, *12*, 313−317.

(22) Hatakeyama, S.; Ohno, M.; Weng, J.; Takagi, H.; Akimoto, H. Mechanism for the formation of gaseous and particulate products from ozone-cycloalkene reactions. *Environ. Sci. Technol.* **1987**, *21*, 52−57.

(23) Kawamura, K.; Gagosian, R. B. Implication of ω−oxocarboxylic acids in the remote marine atmosphere for photo-oxidation of unsaturated fatty acids. *Nature* **1987**, *325*, 330−332.

(24) Ho, K. F.; Lee, S. C.; Cao, J. J.; Kawamura, K.; Watanabe, T.; Cheng, Y.; Chow, J. C. Dicarboxylic acids, ketocarboxylic acids and dicarbonyls in the urban roadside area of Hong Kong. *Atmos. Environ.* **2006**, *40* (17), 3030−3040.

(25) Pavuluri, C. M.; Kawamura, K. New Directions: Need for better understanding of plastic waste burning as inferred from high abundance of terephthalic acid in South Asian aerosols. *Atoms. Environ.* **2010**, *44*, 5320−5321.

(26) Sorooshian, A.; Lu, M.-L.; Brechtel, F. J.; Jonsson, H.; Feingold, G.; Flagan, R. C.; Seinfeld, J. H. On the source of organic acid aerosol layers above clouds. *Environ. Sci. Technol.* **2007**, *41*, 4647−4654.

(27) Fu, T.-M.; Jacob, D. J.; Wittrock, F.; Burrows, J. P.; Vrekoussis, M.; Henze, D. K. Global budgets of atmospheric glyoxal and methylglyoxal, and implications for formation of secondary organic aerosols. *J. Geophys. Res.* **2008**, *113*, D15303 DOI: 10.1029/2007JD009505.

(28) Wittrock, F.; Richter, A.; Oetjen, H.; Burrows, J. P.; Kanakidou, M.; Myriokefalitakis, S.; Volkamer, R.; Beirle, S.; Platt, U.; Wagner, T. Simultaneous global observations of glyoxal and formaldehyde from space. *Geophys. Res. Lett.* **2006**, *33*, L16804 DOI: 10.1029/2006GL026310.

(29) Sorooshian, A.; Varutbangkul, V.; Brechtel, F. J.; Ervens, B.; Feingold, G.; Bahreini, R.; Murphy, S. M.; Holloway, J. S.; Atlas, E. L.; Buzorius, G.; Jonsson, H.; Flagan, R. C.; Seinfeld, J. H. Oxalic acid in clear and cloudy atmospheres: Analysis of data from International Consortium for Atmospheric Research on Transport and Transformation 2004. *J. Geophys. Res.* **2006**, *111* (D23), D23S45.

(30) Wang, X.; Shen, Z.; Cao, J.; Zhang, L.; Liu, L.; Li, J.; Liu, S.; Sun, Y. Characteristics of surface ozone at an urban site of Xi'an in Northwest China. *J. Environ. Monit.* **2012**, *14*, 116−126.

(31) Wang, G.; Chen, C.; Li, J.; Zhou, B.; Xie, M.; Hu, S.; Kawamura, K.; Chen, Y. Molecular composition and size distribution of sugars, sugar-alcohols and carboxylic acids in airborne particles during a severe urban haze event caused by wheat straw burning. *Atmos. Environ.* **2011**, *45*, 2473−2479.

(32) Wang, G.; Kawamura, K.; Umemoto, N.; Xie, M.; Hu, S.; Wang, Z. Water-soluble organic compounds in PM2.5 and size-segregated aerosols over Mt. Tai in North China Plain. *J. Geophys. Res. Atmos.* **2009**, *114*, D19208 DOI: 10.1029/2008JD011390.

(33) Wang, G.; Kawamura, K.; Hu, S.; Xie, M.; Zhou, B.; Li, J.; Cao, J.; An, Z. Selected water-soluble organic compounds found in size-resolved aerosols collected from the urban, mountain, and marine atmospheres over East Asia. *Tellus B* **2011**, *63*, 371−381.

(34) Wang, G.; Kawamura, K.; Xie, M.; Hu, S.; Cao, J.; An, Z.; Watson, J. G.; Chow, J. C. Organic molecular compositions and size distributions of Chinese summer and autumn aerosols from Nanjing: Characteristic haze event caused by wheat straw burning. *Environ. Sci. Technol.* **2009**, *43*, 6493−6499.

(35) Wang, G.; Kawamura, K.; Xie, M.; Hu, S.; Gao, S.; Cao, J.; An, Z.; Wang, Z. Size-distributions of *n*-alkanes, PAHs and hopanes and their sources in the urban, mountain and marine atmospheres over East Asia. *Atmos. Chem. Phys.* **2009**, *9* (22), 8869−8882.

(36) Herner, J. D.; Ying, Q.; Aw, J.; Gao, O.; Chang, D. P. Y; Kleeman, M. J. Dominant mechanism that shape the airborne particle size and composition distribution in central California. *Aerosol Sci. Technol.* **2006**, *40*, 827−844.

(37) Court, J. D.; Goldsack, R. J.; Ferrari, L. M.; Polach, H. A. The use of carbon isotopes in identifying urban air particulate sources. *Clean Air* **1981**, 6−11.

(38) Kawashima, H.; Haneishi, Y. Effects of combustion emissions from the Eurasian continent in winter on seasonal d13C of elemental carbon in aerosols in Japan. *Atmos. Environ.* **2012**, *46*, 568−579.

(39) Hoefs, J. *Stable Isotope Geochemistry*; Springer: New York, 1997.

(40) Pavuluri, C. M.; Kawamura, K. Evidence for 13-carbon enrichment in oxalic acid via iron catalyzed photolysis in aqueous phase. *Geophys. Res. Lett.* **2012**, *39*, L03802 DOI: 10.1029/2011GL050398.